Int. J. Electrochem. Sci., **17 (2022)** Article Number: 221062, doi: 10.20964/2022.10.62

International Journal of
ELECTROCHEMICAL
SCIENCE
www.electrochemsci.org

Influence of Si_3N_4 nanoparticles on morphology, hardness and corrosion resistance of electrodeposited Ni-Co- Si_3N_4

Maryam Tizgadam[1], *Stefan Hengsberger*[1], *Ali Rasooli*[2,*], *Somayeh Ahmadiyeh*[2]

[1] University of Applied Sciences and Arts Western Switzerland, Fribourg, Switzerland
[2] Department of Materials Engineering, University of Tabriz, Tabriz, Iran.
[*]E-mail: a.rasooli@tabrizu.ac.ir

Received: 6 May 2022 / *Accepted:* 30 June 2022 / *Published:* 10 September 2022

The main goal of this study was based on estimating the influence of Si_3N_4 reinforcement nanoparticles on the mechanical and electrochemical properties of Ni-Co-Si_3N_4 nanocomposite coatings. Ni-Co-Si_3N_4 nanocomposite coatings were electrodeposited on copper from a modified Watts bath containing Si_3N_4 particles by direct current (DC). The effect of Si_3N_4nano-particles on the properties of Ni-Co coatings was studied. Surface morphology, chemical composition, grain size and corrosion resistance of Ni-Co and Ni-Co-Si_3N_4 nanocomposite coatings were investigated by scanning electron microscope (SEM), energy dispersive X-ray detector (EDS) coupled with SEM, X-ray diffraction analysis (XRD) and electrochemical impedance measurements, respectively. It was found that surface morphologies of Ni-Co coatings were changed by using nano-particles. There was no difference in the microstructure of coatings, both electrodeposited Ni-Co and Ni-Co-Si_3N_4 nanocomposite coating's crystalline structure was face-centered cubic (FCC). Based on impedance measurements, it revealed that the corrosion resistance of nanocomposite coatings was more than that of electrodeposited Ni-Co coating. The microhardness of the nanocomposite coatings (678 HV) was higher than that of Ni-Co (580 HV) due to dispersion-strengthening and matrix grain refining. The best mechanical and corrosion resistance properties achieved at the Ni-Co-7.9 wt% Si_3N_4 nanocomposite coating.

Keywords: Electrodeposition, Ni-Co-Si_3N_4 nanocomposite coatings, X-ray diffraction Corrosion resistance, microstructural features, microhardness

1. INTRODUCTION

Ni-coatings are among the common metal coatings which are used for various purposes like decorative and protective aims due to their high tensile strength, good toughness, and corrosion resistance. There are several methods for improving the pure Ni-coatings properties, such as reducing the grain size of the coating by applying organic additives, changing current density [1-4], alloy making [5-8] and also the using reinforcement particles [9-11]. Co-deposition and alloy making of Ni, Co and

Fe are very desirable in most industries. Several papers have been published on Ni-Co alloy coatings in different sulfate, chloride and Watts bath with and without additives [12-14]. Various studies show that chemical composition and properties of Ni-Co coatings which are generated by electrical deposition method, depend on bath's chemical composition parameters (concentration of metal ions and additives in the electrolyte) and parameters which are related to electrical deposition (shape and density of current signal) and other parameters like stirring rate and temperature [13-17]. In the last few decades in order to overcome the limitations of metal coatings and also to increase the hardness, wear and corrosion resistance of them, producing of composite coatings, containing ceramic particles in a metal matrix by electrochemical deposition method have been studied. Composite coatings due to their hardness and high tensile strength, good thermal conductivity, and superior magnetic properties are very popular in several industries. There are several reports that investigated the influence of different ceramic particles such as SiO_2 [18-20], TiO_2 [21], Al_2O_3 [22], SiC [23], WC [24] and ZnO [25] on the coatings. Among the various reinforcing particles, Si_3N_4 has been received more attention, due to its high hardness nearly 800-1200 Vickers, hot oxidation resistance and high abrasion resistance. It's expected that by the distribution of Si_3N_4 in Ni-Co matrix the mechanical and corrosion properties will be improved. A few types of researches have been done on the effect of Si_3N_4 nanoparticles on Ni-Co alloy coatings. Kasturibai [26] investigated the corrosion properties of Ni-Si_3N_4 nanocomposite coatings, and Srivastava [27] studied the influence of Co on Si_3N_4 incorporation in electrodeposited Ni-based coatings. Srivastava [28] compared the impact of SiC, Si_3N_4, and Al_2O_3 on the properties of electrodeposited Ni, and Shi [29] studied the effect of Si_3N_4 on tribological properties of Ni-Co coating. In the present study, Si_3N_4 is distributed on the Ni-Co matrix then, mechanical and corrosion properties of Ni-Co-Si_3N_4 nanocomposite coatings are investigated. Also, the influence of Si_3N_4 on Ni-Co coating's structure, morphology, and chemical composition are studied.

2. EXPERIMENTAL

The Ni-Co-Si_3N_4 nanocomposite coatings were deposited on copper plates of size 10×10×1mm as the cathode, by using nickel plate of 40×30×1 mm as the anode which kept apart parallel to them. Before plating, previously polished substrates (mechanically by silicon carbide abrasive papers up to 2500 grit), were decreased by the alkaline solution in 45°C for 5 min in order to remove the impurities. Finally, the substrates were activated in 10%H_2SO_4, for 30 seconds and prior to the electrodeposition process, surfaces were rinsed by distilled water.

Table 1. Watts bath composition for Ni-Co-Si_3N_4 coatings

Materials	Amount in bath (g/l)
Nickel sulfate ($NiSO_4.6H_2O$)	**250**
Nickel chloride ($NiCl_2.6H_2O$)	**40**
Cobalt sulfate ($CoSO_4.7H_2O$)	**40**
Boric acid (H_3BO_3)	**40**
Sodium dodecyl sulfate (SDS) $C_{12}H_{25}NaO_4S$	**0.35**
Silicon nitride particles (Si_3N_4)	**0-30**

The coatings were obtained using Watts baths with different amounts of Si_3N_4 which its compositions are listed in Table 1. All coatings were deposited at the temperature of 45˚C in pH of 4.5 and by applying an optimized direct current density of 4 A/dm^2. After adding Si_3N_4 nanoparticles with 0.35 g/l sodium dodecyl sulfate surfactant (SDS), the electrolyte was stirred continually in a fixed speed by a magnetic stirrer for 24 hours to disperse nanoparticles uniformly and prevent their agglomeration. Finally, in order to have a suitable homogeneous electrolyte, the suspension was agitated by an ultrasonic device (Mercury, turkey) for 20 min just before the deposition. After applying the coatings, microhardness measurements were carried out using a Novo test T8-MCV Microhardness Tester with a load of 50g for 15 sec, and the average of four measurements was reported. The morphology and the phase structure of coatings were studied by FE-SEM Mira Tescan scanning electron microscope (FE-SEM) and D8 ADVANCE-BRUKER AXS X-ray diffractometer. The weight percentage of each element in the coatings was determined by using an energy dispersive X-ray detector (EDS) coupled with FE-SEM. The corrosion resistance of coatings was investigated by electrochemical impedance measurements (EIS) in by OrigaFlex-OGF01 Potentiostat /Galvanostat Company (France) run by the Origalys software.

For establishing the open circuit potential, prior to the electrochemical analysis, the coatings were submerged in the 3.5% NaCl solution for 60 min. All tests were done at room temperature in a typical three-electrode cell. The counter electrode was a platinum sheet with an area of about 10 cm^2, and all potentials were measured vs. a commercial saturated calomel electrode (SCE). The frequency changed from 100 kHz to 10 MHz, and the r.m.s (root mean square) amplitude was ±10 mV. The equivalent circuit has been simulated by Z'view (II) software.

3. RESULTS AND DISCUSSION

3.1 Effect of particle concentration on Morphology of coatings

Figure 1 shows SEM images of the surface morphology of coatings which were obtained from the electrolytes with different concentration of Si_3N_4 nano-particles, in the same deposition condition in 4A/dm^2. It was observed that Ni-Co alloy coating has pyramidal morphology (Fig.1a) formerly. It is reported that cobalt changes the morphology of the nickel coating to spherical [30]. It seems that the mechanism of a growing surface in alloying Ni-Co coatings is such that, first in inactive sites, the spherical masses are germinated, then by the growth of the spherical masses, the structure of coating change to spherical [31]. But in the present study, cobalt doesn't change the morphology of coatings to spherical significantly, it may be related to cobalt concentration in the bath, which Bakhit [32] substantiated in their study on electrodeposited Ni-Co coatings, where the cobalt concentration in the electrolyte is under 40g/l, the morphology of coating remains pyramidal. Therefore, it can be concluded that in the present work, because the concentration of cobalt in the bath is 40g/l, the obtained Ni-Co coatings just have a slight tendency to spherical morphology. It was seen that by adding Si_3N_4 nanoparticles to the electrolyte, the morphology becomes a bit spherical (Fig. 1b); however, pyramid morphology was observed in some areas (Fig. 1 c-d).

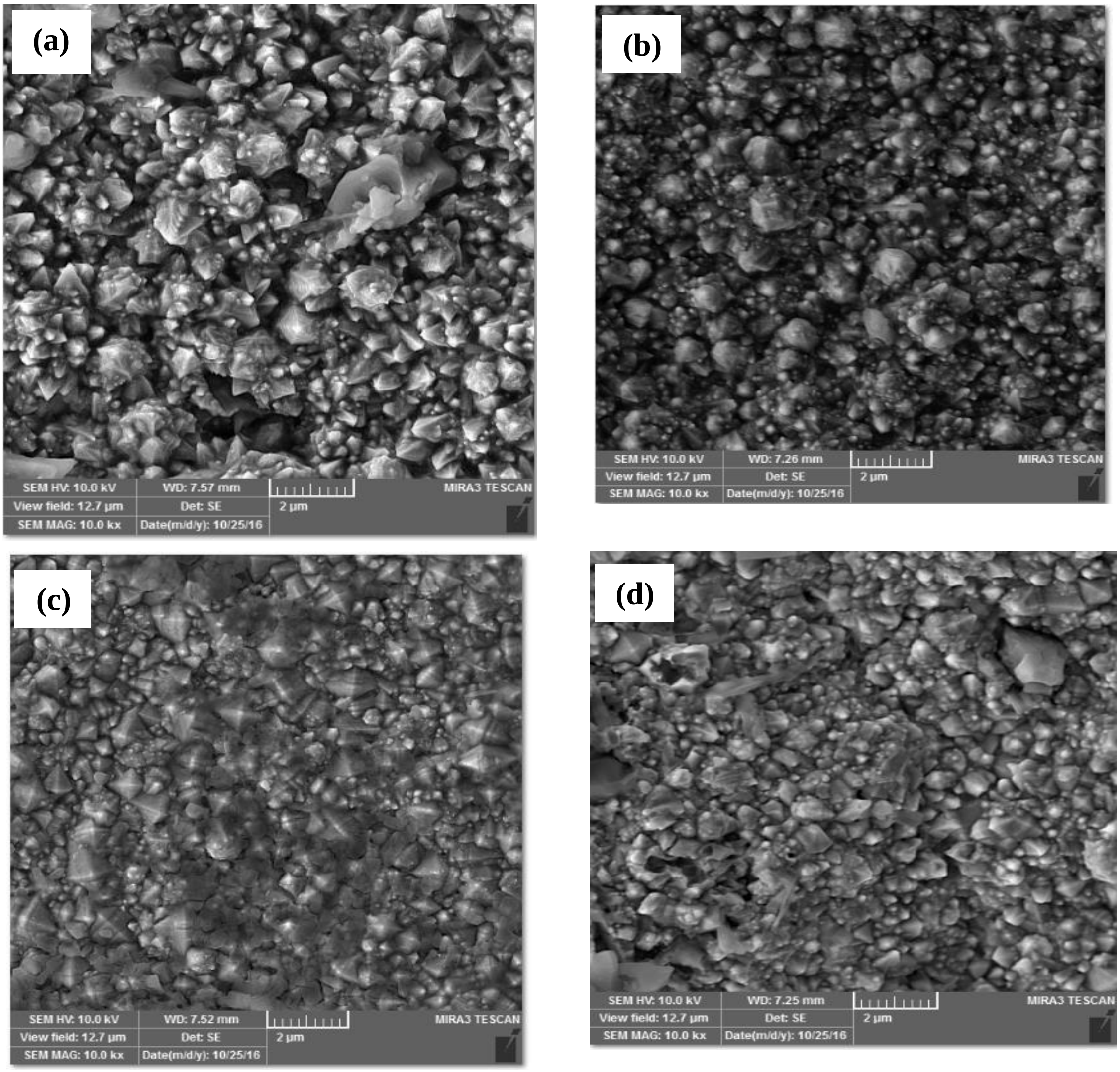

Figure 1. Surface morphology of Ni-Co (a), Ni-Co- (5g/l) Si_3N_4 (b), Ni-Co- (15g/l) Si_3N_4 (c), Ni-Co- (30g/l) Si_3N_4 (d) coatings in current density of $4A/dm^2$

According to previous research [33], well-distributed nanoparticles in a Ni-Co matrix inhibit growing of the pyramids. It seems that the co-deposition mechanism of Si_3N_4 nanoparticles is in accordance with Guglielmi's theory [34]. Where Si_3N_4 nanoparticles are absorbed initially and weakly by electrophoresis forces on the peak of the pyramids (active sites), and the growth process of pyramids is retarded. Then, deposition of metallic cations on nanoparticles leads to strong absorption of particles hence new suitable sites for germination are created. Continuing these three steps, result in the formation of spherical morphology. It was observed from Fig. 1 (b-d) that, although the Si_3N_4 nanoparticles concentration in the bath were increased from 5 to 30g/l, the portion of spherical morphology was reduced due to particles agglomeration. Kasturibai [26], Srivastava [27] and Shi [29] mentioned the agglomeration of nanoparticles in nanocomposite coatings for higher concentrations.

3.2 EDS spectra analysis

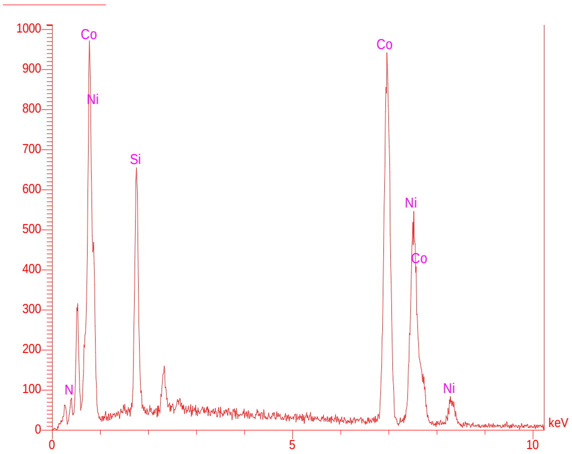

Figure 2. EDAX analysis spectrum of electrodeposited Ni-Co- (5g/l) Si_3N_4 coating.

Fig. 2 shows the EDS spectra of Ni-Co-Si_3N_4 nanocomposite coating which obtained by the addition of 5g/l Si_3N_4 to bath in current density of 4A/dm^2. The presence of Si peak in the EDS spectrum confirms that Si_3N_4 nanoparticles are co-deposited in the Ni-Co matrix. The weight percentage of all elements in the coating is calculated by using the EDS spectra's datum and given in table2.

Table 2. Weight percentage of elements in coating

Coating	Ni (wt. %)	Co (wt. %)	Si (wt. %)	N (wt. %)
Ni- Co	45.51	53.69	0	0
Ni-Co-Si_3N_4 (5g/l)	36.09	56.01	4.6	3.3
Ni-Co-Si_3N_4 (15g/l)	37.94	55.12	3.8	3.14
Ni-Co-Si_3N_4 (30g/l)	39.67	53.65	3.2	3.048

3.3 Effect of Si_3N_4 concentration on the chemical composition of the coating

The effect of Si_3N_4 concentration in the bath on the chemical composition of the coating is shown in table 2 and Fig.3. It's observed from table2 that by adding 5g/l Si_3N_4 to the electrolyte, the weight percentage of co-deposited cobalt was increased from 53.69 wt. % in Ni-Co alloy coating to 56.01wt. % in the Ni-Co-Si_3N_4 nanocomposite coating. It's also shown in table 2 that for all concentrations of Si_3N_4 in the bath, the weight percentage of cobalt is more than that of nickel. This is because of anomalous co-deposition of Ni-Co, which in such processes, the less noble metal is deposited preferentially [35]. There are several mechanisms for explaining the anomalous co-deposition of Ni-Co. Qiao [16] reported that the reason for anomalous co-deposition of Ni-Co is a result of the significant decrease in cobalt ions through the diffusion layer due to the higher tendency of these ions to be absorbed in the cathode surface.

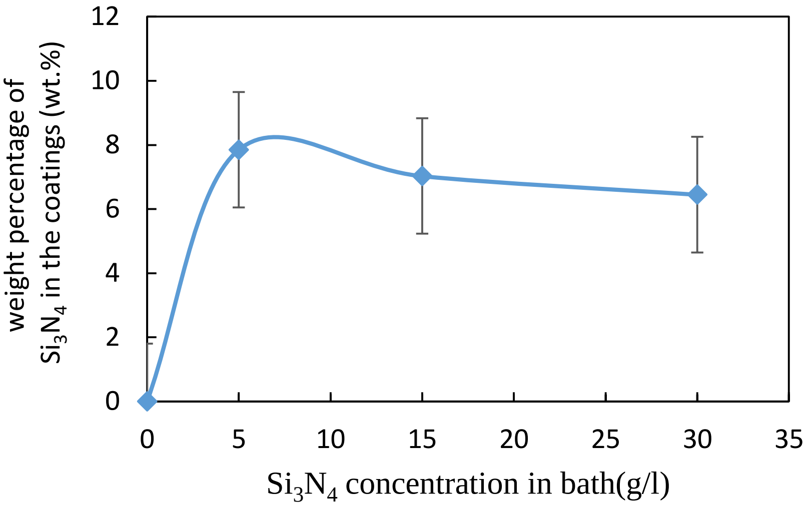

Figure 3. Effect of **Si_3N_4** concentration on the weight percentage of **Si_3N_4** in coatings.

Where, by increasing the concentration of cobalt in the electrolyte, in order to compensate for the decreasing cobalt ions, the amount of cobalt in the alloy coatings increased. Gomez [36] presented that in an anomalous co-deposition of Ni-Co, after deposition of Ni ions, the Co ions deposit on nickels and prevent the reduction of other Ni ions. Bai and Hu [37] suggested that anomalous co-deposition of Ni-Co is because of the formation and absorption of metal hydroxides near the cathode due to the increasing pH in cathode proximity. They showed that due to the more tendency of cobalt hydroxides than nickel hydroxides to be absorbed on the cathode surface, the amount of cobalt deposit in the matrix is higher. Beyond 5g/l Si_3N_4, by increasing the Si_3N_4 concentration to 30 g/l, the weight percentage of co-deposited cobalt decreased to 53.70 wt. %. It is reported that [32] in composite electrodeposition, cobalt deposits in two ways, first by direct reduction of cobalt ions through the electrolyte on the cathode's surfaces and second by reduction of cobalt ions on the surfaces of the particles which are adsorbed on the cathode's surface. Therefore, by adding nanoparticles to the bath up to an optimum level, the weight percentage of cobalt in the coatings is increased due to its simultaneous reduction both on the cathode surface and newly added particle surfaces. Actually, beyond 5g/l Si_3N_4, the reduction of cobalt ions on the surface of the particles is not noticeable as their direct reduction on the cathode's surface.

It's observed from Fig.3 that by increasing the Si_3N_4 concentration in the bath from 5 to 30 g/l, the amount of co-deposited Si_3N_4 were decreased from 7.85 to 6.45 wt. %. Similar results have been reported by other researchers. Kasturibai and Kalaigna [26] reported that co-deposited particles were increased by increasing the Si_3N_4 concentration in the bath from 3 to 12 g/l, and beyond this amount the weight percentages of Si_3N_4 were decreased. The reason for the decreasing of co-deposited particles is the agglomeration of nano-sized particles in the solution. Aal [38] also represented that the decreasing of co-deposited particles in the high concentration of particles in the bath due to the formation of agglomerated particle's film on the surface of the cathode, which stopped the resuming of particles co-deposition.

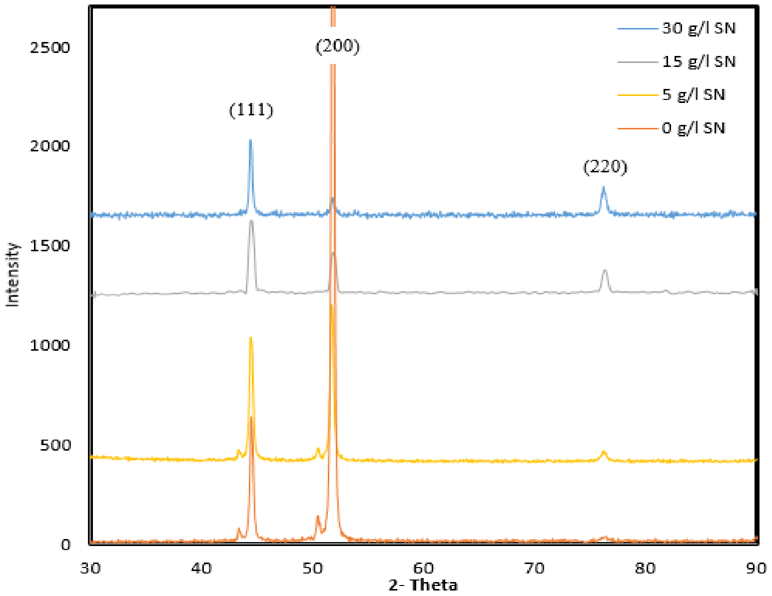

Figure 4. XRD diffraction of Ni-Co (a), Ni-Co- (5g/l) Si_3N_4 (b), Ni-Co- (15g/l) Si_3N_4 (c), Ni-Co- (30g/l) Si_3N_4(d) coatings in current density of $4A/dm^2$

3.4 X-ray diffraction analysis

For the studies of the phase structure of Ni-Co and Ni-Co-Si_3N_4 coatings, XRD patterns of deposits are shown in fig4. It is observed that the presence of Si_3N_4 nanoparticles doesn't change the crystalline structure of the coatings. Therefore, the structure of both Ni-Co alloying coating and Ni-Co-Si_3N_4 nanocomposite coatings is FCC. The peaks that are shown in these patterns refer to (111), (200) and (220) which confirm that the structure of coatings is FCC. There are no peaks of Si_3N_4 due to its low content in coatings. It's seen that, however, the position of peaks wasn't altered by increasing Si_3N_4 concentration in the bath from 5 to 30g/l Si_3N_4, the intensity was decreased for (200) and (111) and was increased for (220). These observations revealed that the preferential growth orientation of the Ni-Co matrix is influenced by Si_3N_4 nano-particles and changed to (220). Based on the Ni-Co phase diagram, up to 66 wt.% Cobalt, all of the obtained coatings have the structure of α (alpha) single phase region [39].

The crystal sizes of the coating were calculated by using the Scherrer's equation [40] which is given below, where FWHM is the full-width half maxima in $2\theta^{\circ}$, D the crystallite size nanometers, K= 0.94 is constant, and λ=0.154 nm is the wavelength of CuKα radiation.

$$FWHM = \frac{K\lambda}{D\ cos\theta}\frac{180^0}{\pi} \qquad (1)$$

Measured crystallite sizes calculated from Scherrer's equation are given in table 3.

Table 3. The crystallite size of Ni–Co based coatings.

Coating	Grain size (nm)
Ni-Co	30.74
Ni-Co-5g/l Si_3N_4	26.33
Ni-Co-15 g/l Si_3N_4	29.30
Ni-Co-30 g/l Si_3N_4	29.87

It is found that the crystallite size of the coatings was decreased by the addition of the nanoparticles, where the crystallite size of Ni-Co was 30.74 nm, and the crystallite size of Ni-Co-5g/l Si_3N_4 was 26.33 nm. The reason for the crystallite size decreasing in the presence of nanoparticles is that Si_3N_4 particles in the interface of the growth metal/ electrolyte inhibit the growth of crystal and make it more compact. Also, the Si_3N_4 particles are suitable sites for the heterogeneous nucleation and cause to the reduction in crystallite size [19, 20, 25]. By increasing the Si_3N_4 to 15 g/l concentration in bath the crystallite size increase from 26.33nm to 29.87nm, because by increasing the Si_3N_4 concentration in the bath the nanoparticles are agglomerated, thus the weight percentage of particles in coatings is decreased and consequently, the influence of particles on crystallite size decreases.

3.5 Effect of particle concentration on microhardness

The influence of nanoparticles on microhardness of coatings is shown in Fig.5. It's observed that the microhardness of nanocomposite coatings is much larger than that of the Ni-Co alloy coating (580 Vickers). The coating with 5g/l Si_3N_4 in the bath displays the highest microhardness of 678 Hv. By increasing the bath loading from 5g/l to30 g/l Si_3N_4 and reducing the Si_3N_4 reinforcement particles content of in the deposits, the microhardness of nanocomposite coatings was decreased from 678 to 606 Hv. It's confirmed that 5g/l Si_3N_4 as the second phase has reduced the crystal size of coatings, so according to the Hall-Petch relation, 5g/l Si_3N_4 cause to increase the microhardness of Ni-Co coatings. Also, due to the Orowan mechanism nanoparticles immobilize the dislocations and grain boundaries and hinder the plastic deformation. It is understood from Shi [29] and kasturibai [26] researches that the microhardness of composite coatings depends directly to nanoparticle content in coatings whereby the increasing amount of nanoparticle in the coating the microhardness increased due to Hall-Petch and Orowan mechanisms.

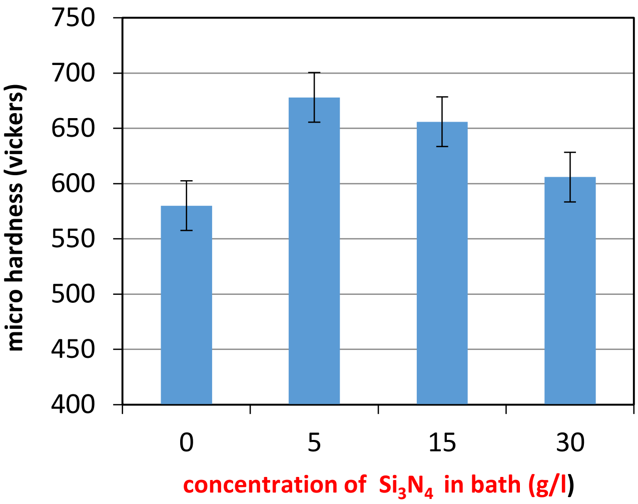

Figure 5. The micro hardness of Ni-Co- Si_3N_4 in different concentration of Si_3N_4 produce in current density of 4A/dm^2

3.6 Electrochemical impedance measurements

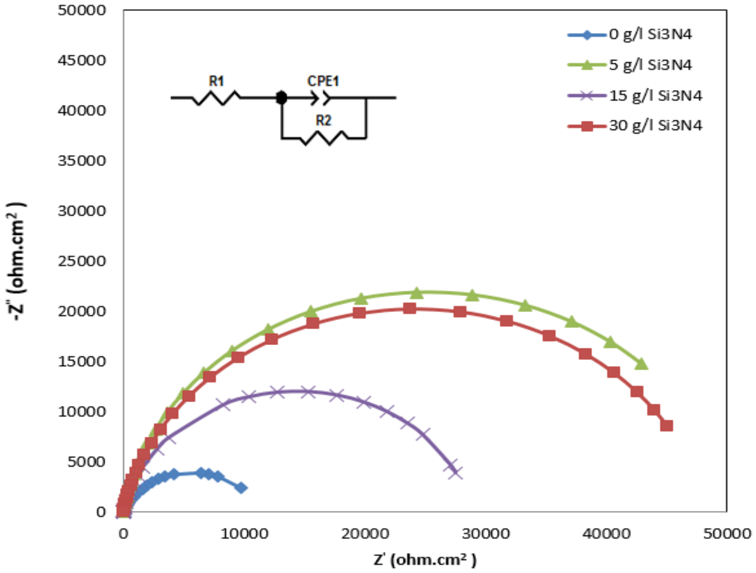

Figure 6. Nyquist impedance diagrams and the equivalent electrical circuit model for Ni-Co coating and Ni-Co-Si_3N_4

The Nyquist curves which are obtained from Electrochemical impedance measurements for the electrodeposited Ni-Co and Ni-Co-Si_3N_4 nanocomposite coatings and also the equivalent electrical circuit model for coatings in 3.5 wt.% NaCl aqueous solution at ambient temperature is shown in Fig.6, where R_1 is the solution resistance, R_2 is charge transfer resistance that determines the electron transferring through the coating and it is related inversely to corrosion rate, CPE is a constant phase element. Table 3 reveals information extracted from the Electrochemical impedance measurements.

It's observed that there is a noticeable difference between the impedance values of Ni-Co alloying coating and Ni-Co-Si_3N_4 nanocomposite coatings, in which the corrosion resistance of coatings (R_2)

significantly increases from 11357 ohm.cm^2 for alloy coating to 50459 ohm.cm^2 for Ni-Co-5g/l Si_3N_4 composite coating (contains 56.01 wt.% Co and 7.85 wt.% Si_3N_4). This deposit displays the highest corrosion resistance among the other coatings. Actually, nanoparticles with different mechanisms can improve the corrosion resistance of composite coatings. These particles can change the effective surface area, in a way that the nonconductive particles reduce and the conductive particles increase the effective surface area [30]. Si_3N_4 is known as nonconductive material that its electrical resistance is $10^{13}\Omega$, thus its incorporation in Ni-Co matrix leads to effective surface area decrease and hence more corrosion resistance. Also, by distributing particles uniformly in the matrix the micro-galvanic cells at particle/matrix interfaces were formed which they can alter the mechanism of corrosion from localized corrosion and pitting corrosion to homogenous corrosion [41]. Shi [29] reported a similar result for Ni-Co-Si_3N_4 coating, in addition, the doping of nanoparticles reduces the preferential locations for corrosion initiation by filling the nano-scale gaps and cracks [39, 42, 43].

Table 4. Electro chemical impedance measurement's information.

Coating	R_2 (ohm.cm^2)	R_1 (ohm.cm^2)	CPE-P	CPE-T (f.cm$^{-2)}$	sum of squared
Ni-Co	11357	3.654	0.7789	0.00022	0.97716
Ni-Co- Si_3N_4 (5 g/l)	50459	4.346	0.91056	9.01E-0.5	0.12187
Ni-Co- Si_3N_4 (15 g/l)	28826	3.315	0.88514	5.98E-0.5	0.98057
Ni-Co- Si_3N_4 (30 g/l)	48324	5.844	0/88748	4.81E-0.5	0.3539

Table 5. Weight percentage of Co and Si_3N_4 in coatings.

Coating	Co (wt. %)	Si_3N_4 (wt. %)	R_2 (ohm.cm^2)
Ni- Co	53.69	0	11357
Ni-Co-Si_3N_4 (5g/l)	56.01	7.85	50459
Ni-Co-Si_3N_4 (15g/l)	55.12	7.03	28826
Ni-Co-Si_3N_4 (30g/l)	53.7	6.45	48324

It is evident in Table 4 that by decreasing the weight percentage of Si_3N_4 in nanocomposite coatings (increasing the concentration of Si_3N_4 in the bath) the corrosion resistance of coatings was somehow decreased. Comparing results of two samples which are deposited in bathes contain 15 g/l Si_3N_4 and 30 g/l Si_3N_4 observed that although the weight percentage of Si_3N_4 in coating 15 g/l Si_3N_4 is more than it in 30 g/l Si_3N_4, the corrosion resistance of 15 g/l Si_3N_4 is less than 30 g/l Si_3N_4. This behavior is subjected to a higher weight percentage of cobalt in compare with the Si_3N_4 slight deficit. As shown in table5, the weight percentage of cobalt in 30 g/l Si_3N_4 is less than 15 g/l Si_3N_4. Earlier [44] observations are shown that, by increasing the weight percentage of cobalt in coatings, the corrosion resistance was decreased. Due to the Standard Electrode potentials, cobalt is less noble than Nickel, therefore by increasing the weight percentage of cobalt in coatings, the corrosion resistance of coatings was decreased. So it could be concluded that not only the weight percentage of Si_3N_4 but also the ratio of cobalt's weight percentage per Si_3N_4 weight percentage in coatings Plays an important role in the corrosion resistance of Ni-Co-Si_3N_4 coatings.

4. CONCLUSION

1- Ni-Co and Ni-Co-Si_3N_4 nanocomposite coatings were successfully deposited in the modified Watts bath. Presence of 5g/l Si_3N_4 in bath cause to spherical morphology of coating. By increasing the concentration of Si_3N_4 from 5 to 30 g/l, the agglomerated nanoparticles on surface morphology were visible

2- The Ni-Co-Si_3N_4 nanocomposite which carried out in the current density of 4A/dm^2 and in the bath with 5g/l Si_3N_4 had a maximum weight percentage (7.85wt. %) of Si_3N_4 in the coating which it causes to good mechanical properties and also corrosion resistance of coatings. By increasing the concentration of Si_3N_4, due to the agglomeration of nanoparticles, the weight percentage of Si_3N_4 in coating decreased. Also adding 5 g/l Si_3N_4, resulted in increasing the cobalt's weight percentage in the coating from 53.69 to 56.01 wt. %. In the high concentration of nanoparticles, the weight percentage of cobalt decrease to 53.70 wt. %.

3- The structure of coatings was FCC, which means, disturbed Si_3N_4 particles in the Ni-Co matrix didn't change the crystalline structure of coatings, but preferred growth orientation and crystal sizes of coatings were influenced by Si_3N_4 nano-particles. Where the preferred growth orientation changed from (200) to (111) and the crystal sizes of coatings decreased from 30.74nm in Ni-Co Alloy coating to 26.33nm in Ni-Co-7.85 wt.% Si_3N_4. By decreasing the weight percentage of Si_3N_4 in the coating, the crystal sizes of the coating increased to 29.87nm.

4- The reinforcement of Si_3N_4 in the composite coating improved the microhardness of coatings. In 7.85 wt. % Si_3N_4, the microhardness increased from 580 (in Ni-Co Alloy coating) to 678 Vickers.

5- The significant difference in corrosion resistance of Ni-Co and nanocomposite coatings of Ni-Co-Si_3N_4 were observed in the electrochemical study of the deposits. Where Ni-Co-Si_3N_4 nanocomposite obtained from the electrolyte containing 5 g/l Si_3N_4, has the best corrosion resistance (50459 ohm.cm^2) in the comparison with Ni-Co alloying coating (11357 ohm.cm^2).

6- Finally, it can be concluded that the Ni-Co-Si_3N_4 nanocomposite which carried out in current density of 4 A/dm^2 and in the bath with 5 g/l Si_3N_4 has the maximum weight percentage of Si_3N_4 in the coating which it causes to good mechanical properties and also corrosion resistance of coatings.

ACKNOWLEDGEMENT
The authors would like to acknowledge the financial support of the Office of Vice Chancellor in Charge of Research of the University of Tabriz.

References

1. A.M. Rashidi and A. Amadeh, *Surf. Coat. Technol.*, 202 (2008) 3772-3776.
2. L.P. Bicelli, B. Bozzini, C. Mele and L. D'Urzo, *Int. J. Electrochem. Sci.*, 3 (2008) 356 - 408.

3. J.-X. Kang, W.-Z. Zhao and G.-F. Zhang, *Surf. Coat. Technol*., 203 (2009) 1815-1818.
4. Y.F. Shen, W.Y. Xue, Y.D. Wang, Z.Y. Liu and L. Zuo, *Surf. Coat. Technol*., 202 (2008) 5140-5145.
5. O. Hammami, L. Dhouibi and E. Triki, *Surf. Coat. Technol*., 203 (2009) 2863-2870.
6. N. Eliaz, T.M. Sridhar and E. Gileadi, *Electrochim. Acta*, 50 (2005) 2893-2904.
7. A. Naor, N. Eliaz and E. Gileadi, *Electrochim. Acta*, 54 (2009) 6028-6035.
8. E. Beltowska-Lehman, *Surf. Coat. Technol*., 151-152 (2002) 440-443.
9. A.C. Ciubotariu, L. Benea, M. Lakatos–Varsanyi and V. Dragan, *Electrochim. Acta*, 53 (2008) 4557-4563.
10. M. Lekka, N. Kouloumbi, M. Gajo and P.L. Bonora, *Electrochim. Acta*, 50 (2005) 4551-4556.
11. C.S. Lin, C.Y. Lee, C.F. Chang and C.H. Chang, *Surf. Coat. Technol*., 200 (2006) 3690-3697.
12. W.E.G. Hansal, B. Tury, M. Halmdienst, M.L. Varsányi and W. Kautek, *Electrochim. Acta*, 52 (2006) 1145-1151.
13. E. Gómez, S. Pané, X. Alcobe and E. Vallés, *Electrochim. Acta*, 51 (2006) 5703-5709.
14. S. Hassani, K. Raeissi and M.A. Golozar, *J. Appl. Electrochem*., 38 (2008) 689-694.
15. D. Golodnitsky, Y. Rosenberg and A. Ulus, *Electrochim. Acta*, 47 (2002) 2707-2714.
16. G. Qiao, T. Jing, N. Wang, Y. Gao, X. Zhao, J. Zhou and W. Wang, *Electrochim. Acta*, 51 (2005) 85-92.
17. R. Oriňáková, A. Oriňák, G. Vering, I. Talian, R.M. Smith and H.F. Arlinghaus, *Thin Solid Films*, 516 (2008) 3045-3050.
18. W. Sassi, L. Dhouibi, P. Berçot and M. Rezrazi, *Appl. Surf. Sci*., 324 (2015) 369-379.
19. S.I. Ghazanlou, S. Ahmadiyeh and R. Yavari, *Surf. Eng*., 33 (2017) 337–347.
20. S.I. Ghazanlou, A.H.S. Farhood, S. Hosouli, S.Ahmadiyeh and A. Rasooli, Mater. Manuf. Processes., DOI 10.1080/10426914.10422017.11364748(2017).
21. W. Chen, W. Gao and Y. He, *Surf. Coat. Technol*., 204 (2010) 2493-2498.
22. J. Feng, M.G.S. Ferreira and R. Vilar, *Surf. Coat. Technol*., 88 (1997) 212-218.
23. Shawki, Saher and Z.A. Hamid, *Anti-corrosion methods and materials*, 44.3 (1997) 178-185.
24. Y. Wang and Z. Xu, *Surf. Coat. Technol*., 200 (2006) 3896-3902.
25. G. SI, F. AHS, H. S, A. S and R. A., *J. Mater. Sci.: Mater. Electron*., 28 (2017) 15537-15551.
26. S. Kasturibai and G.P. Kalaignan, *Bull. Mater. Sci*., 37 (2014) 721-728.
27. M. Srivastava, V.K.W. Grips and K.S. Rajam, *J. Alloys Compd.*, 469 (2009) 362-365.
28. M. Srivastava, V.K. William Grips and K.S. Rajam, *Mater. Lett*., 62 (2008) 3487-3489.
29. L. Shi, C.F. Sun, F. Zhou and W.M. Liu, *Science and Engineering*: A, 397 (2005) 190-194.
30. L. Wang, Y. Gao, Q. Xue, H. Liu and T. Xu, *Appl. Surf. Sci*., 242 (2005) 326-332.
31. B. Tury, G.Z. Radnóczi, G. Radnóczi and M.L. Varsányi, *Surf. Coat. Technol*., 202 (2007) 331-335.
32. B. Bakhit, Advanced Materials Research Center, Faculty of Materials Engineering, Sahand University of Technology, Tabriz, Iran, 2010.
33. B. Bakhit and A. Akbari, *Surf. Coat. Technol*., 253 (2014) 76-82.
34. N. Guglielmi, *Journal of the Electrochemical Society*, 119.8 (1972) 1009-1012.
35. A. Brenner, Electrodeposition of alloys: principles and practice, Academic Press, (2013) New York.
36. E. Go´mez, J. Ramirez and E. Valle´s, *J. Appl. Electrochem*., 28 (1998) 71-79.
37. A. Bai and C.-C. Hu, *Electrochim. Acta*, 47 (2002) 3447-3456.
38. A.A. Aal, K.M. Ibrahim and Z.A. Hamid, Wear, 260 (2006) 1070-1075.
39. Y. Wang, S.L. Tay, S. Wei, C. Xiong, W. Gao, R.A. Shakoor and R. Kahraman, *J. Alloys Compd*., 649 (2015) 222-228.
40. B.D. Cullity and J.W. Weymouth., *American Journal of Physics*, 25.6 (1957) 394-395.
41. Q. Feng, T. Li, H. Teng, X. Zhang, Y. Zhang, C. Liu and J. Jin, *Surf. Coat. Technol*., 202 (2008) 4137-4144.
42. B. Bakhit, *Surf. Coat. Technol*., 275 (2015) 324-331.
43. A. Rasooli, M.S. Safavi and M. Kasbkar Hokmabad, Ceram. Int., DOI

https://doi.org/10.1016/j.ceramint.2018.01.044.
44. J. Edwards, Coating and surface treatment systems for metals: a comprehensive guide to selection, ASM International, (1997) Materials Park, OH United States